A polo-like kinase modulates cytokinesis and flagella biogenesis in Giardia lamblia

Eun-Ah Park
Yonsei University College of Medicine
Juri Kim
Yonsei University College of Medicine
Mee Young Shin
Yonsei University College of Medicine
Soon-Jung Park (sjpark615@yuhs.ac)
Yonsei University College of Medicine

Research

Keywords: Giardia lamblia, Polo-like kinase, Cell cycle

Posted Date: June 12th, 2020

DOI: https://doi.org/10.21203/rs.3.rs-34665/v1

Abstract

Background

Polo-like kinases (PLKs) are conserved serine/threonine kinase, regulating cell cycle. *Giardia lamblia* PLK (GlPLK) role in its cell has not been yet studied. Here, the function of GlPLK was investigated to provide the insight of roles in *Giardia* cell division, especially during cytokinesis and in flagella formation.

Methods

To access the function of GlPLK, *Giardia* trophozoites were treated with PLK-specific inhibitor, GW843286X (GW) or anti-*glplk* morpholino, then growth of the cells was monitored and phenotypic characteristics of GlPLK-inhibited cells were observed by using mitotic index and flow cytometry assay. Transgenic *G. lamblia* expressing GlPLK as a hemagglutinin (HA)-tagging was constructed and used for immunofluorescence assay to detect the localization of GlPLK, followed by the subcellular fractionation. Furthermore, kinase assay was performed to assess the phosphorylation activities of GlPLK by purified proteins or in vitro synthesized proteins. To elucidate the role of phosphorylated GlPLK, the phosphorylation residues were mutated and expressed in *Giardia* trophozoites.

Results

After incubating trophozoites with 5 μM GW, the percentages of cells with four nuclei and/or longer flagella were increased. Immunofluorescence assays indicated that GlPLK was mainly localized at basal bodies and transiently localized at mitotic spindles in the dividing cells. Fractionation experiments demonstrated that GlPLK is present in the nuclear fraction, as did the centromeric histone H3. Morpholino-mediated GlPLK knockdown resulted in the same phenotypes as those observed in GW-treated cells, i.e., increased mitotic index and flagella length. Kinase assays using mutant recombinant GlPLKs indicated that mutation at Lys51 or at both Thr179 and Thr183 resulted in loss of kinase activity. *Giardia* expressing these mutant GlPLKs also demonstrated defects in cell growth, cytokinesis, and flagella.

Conclusions

These data indicated that GlPLK plays roles in *Giardia* cell division, especially during cytokinesis, and in flagella formation.

Background

Giardia lamblia is a human pathogen that causes diarrheal outbreaks; it is present as either a cyst or a trophozoite. Trophoziotes, the multiplying form found in hosts, possesses a structure that seems to be bilaterally symmetrical in the side view and exhibits asymmetrical polarity in the anterior/posterior and dorsal/ventral views. These cells have two nuclei and cytoskeletal structures, including an adhesive disc, a median body, and four pairs of flagella [1].

Limited information is available regarding the mechanism responsible for regulating the division of *Giardia* trophozoites. It has been reported that *G. lamblia* has defective cell cycle checkpoints, because the cell cycle of *Giardia* trophozoites can progress despite blocked DNA synthesis, double-stranded DNA breaks, or defective mitotic spindles [2]. *In vitro* cultures of *Giardia* trophozoites were dominated by cells at the G2/M-phase [3]. Investigations using synchronized cell cultures with chemicals or counterflow centrifugal elutriation revealed *Giardia* proteins showing phase-specific expression [3, 4, 5]. Interestingly, a study using live imaging of *Giardia* indicated that cytokinesis occurs 60-times faster than in mammalian cells, and that *G. lamblia* uses flagella-mediated membrane tension instead of myosin-dependent contractile rings to initiate daughter cell separation [6].

In mammals, cell division is a complex and well-organized process that incorporates a multitude of protein interactions and macromolecular machineries [7]. This process should be finely and dynamically controlled via the actions of interconnected signaling cascade including aurora kinase (AK), polo-like kinase (PLK), and cyclin-dependent kinase 1 (CDK1) [8]. PLK, a key regulator in this process, has diverged into five paralogues in mammals, i.e., PLK1-5 [9]. Particularly, PLK1 is a mitotic kinase with multiple roles in several steps from G2 to the final step of cytokinesis [10]. These Ser/Thr kinases are defined by the presence of an N-terminal kinase domain (KD) and additional domains, termed polo-box domains (PBDs), which engage in protein interactions [11]. To perform its functions, PLK must be activated and dynamically recruited to distinct subcellular structures spatially and temporally via its interaction with the PBD [12].

The database of *G. lamblia* does indicate an open-reading frame (ORF) for PLK (GL50803_104150). In this study, the putative role of PLK was examined using a PLK inhibitor as well as morpholino-mediated knockdown with respect to cell division of *G. lamblia*. The auto-phosphorylation activity of *G. lamblia* PLK1 (GlPLK1) was measured *in vitro*, and its role in cell division was also confirmed *in vivo* using transgenic *G. lamblia* ectopically expressing a mutant GlPLK1 that lacks critical residue(s) for auto-phosphorylation.

Methods

Culture of G. lamblia trophozoites

G. lamblia trophozoites (strain WB, ATCC30957; American Type Culture Collection, Manassas, VA, USA) were grown in modified TYI-S33 medium (2% casein digest, 1% yeast extract, 1% glucose, 0.2% NaCl, 0.2% L-cysteine, 0.02% ascorbic acid, 0.2% K_2HPO_4, 0.06% KH_2PO_4, 10% calf serum and 0.5 mg/mL bovine bile, pH 7.1) at 37 °C [13].

Scoring of G. lamblia cells for cell growth

IC_{50} was determined by treating *Giardia* trophozoites (2×10^4 cells/mL) with various concentrations of the PLK inhibitor, GW843682X (GW; Cayman Chemical, Ann Arbor, MI, USA) (5–5 μM). After treatment for 24 h, the number of parasites per milliliter was determined using a hemocytometer. As a control, *Giardia* trophozoites were treated with 0.05% DMSO.

Various *Giardia* cells (trophozoites carrying pKS-3HA.neo, pGlPLK.pac, pGlPLKK51R.neo, or pGlPLKT179AT183A.neo) were inoculated into modified TYI-S33 medium at 2×10^4 cells/mL, and the cell numbers were counted every 24 h up to 96 h using a hematocytometer.

Flow cytometry

Both the GW-treated and control *G. lamblia* cells were analyzed for their DNA content using flow cytometry [14]. Briefly, the harvested cells were re-suspended in 50 μL TYI-S-33 culture medium and treated with 150 μL cell fixative (1% Triton X-100, 40 mM citric acid, 20 mM dibasic sodium phosphate, and 200 mM sucrose, pH 3.0) at room temperature for 5 min. The samples were diluted with 350 μL diluent buffer (125 mM $MgCl_2$ in phosphate-buffered saline [PBS: 137 mM NaCl, 2.7 mM KCl, 10.1 mM Na_2HPO_4 and 2 mM KH_2PO_4, pH 7.4]) and then stored at 4 °C until use. Fixed cells were treated with 2.5 μg RNase A (Sigma-Aldrich, St. Louis, MO, USA) and 10 μg/mL propidium iodide (Sigma-Aldrich) for 30 min at 37 °C. The cells were evaluated with respect to their DNA content by flow cytometry followed by analysis with FlowJo software (FlowJo Llc, Ashland, OR, USA).

Flow cytometry of various *Giardia* cells (DMSO-treated control, nocodazole-treated cells, and nocodazole/aphidicolin-treated cells) was performed to examine the ploidy of their genomic DNA.

Mitotic index

To evaluate the role of PLK in cytokinesis in *Giardia*, the ratio of cells with two nuclei to those with four nuclei was compared among DMSO-treated and GW-treated groups, as previously described [15]. Briefly, the cells attached on coverslips were fixed with pre-chilled 100% methanol at -20 °C for 10 min and then air-dried. The cells were then mounted in VECTASHIELD Anti-fade Mounting Medium with 4',6-diamidino-2-phenylindole (DAPI; Vector Laboratories, Burlingame, CA). The number of cells with four or two nuclei was counted in 200 cells per condition.

Microscopy-based observation of Giemsa-stained cells

The cells were attached to slides, air-dried, and fixed with 100% methanol for 10 min. They were then stained with 10% Giemsa solution for 40 min and washed with distilled water. After mounting with dibutyl phthalate xylene (Sigma-Aldrich), the slides were observed with an Axiovert 200 microscope (Carl Zeiss, Oberkochen, Germany).

To determine the mitotic index, the number of cells with four or two nuclei was counted in 200 cells per condition. The effect of GW on cytokinesis was monitored, as described previously [6], based on the following phenotypes: disorganized cytokinesis, defective furrow formation, defective cytokinesis, and failed abscission.

G. lamblia cells stained with Giemsa were also used to observe the effect of GW on flagella formation. Specifically, the length of the caudal flagella was measured using ZEN 2011 (Blue edition, Carl Zeiss).

Construction of G. lamblia expressing HA epitope-tagged GlPLK proteins

A 2,137-bp DNA fragment of the *glplk* gene, which comprises the promoter region (100-bp) and the ORF, was amplified from *Giardia* genomic DNA by PCR using two primers, PPLK-F and PLK-HAX3-R (Table 1). The *Hind*III and *Not*I sites were used for cloning into the plasmid pGFP.pac [16] to obtain pGlPLK.pac. The construct was confirmed by DNA sequencing by a sequencing service company (Macrogen, Seoul, Korea).

Table 1
Primers and morpholino used in this study

Name (GiardiaDB ID)	Nucleotide sequence (5'-3')[a, b]
Transgenic *G. lamblia* expressing HA-tagged GlPLK	
PPLK-F (GL50803_104150)	CATCAAGCTTTCGGGGCTCGCACCCGCTTCC
PLK-HAX3-R (GL50308_104150)	GTTACGCGGCCGCTTA*AGCGTAATCTGGAACATCGTATGGGTAAGCGTAATCTGGAACATCGTATGGGTAAGCGTAATCTGGAACATCGTATG*
Pplk-F	CATCGCGGCCGCGTAGGCGTCATCCGAGGTGAAC
PLK-NL-R	GTTACGTCGACGTCTATTTGTGGATACTCGGCTT
Pplk-R	GTTACAAGCTTGGGGCTATAAAATTTTACAGAG
PLK-PBD-F	GTTACAAGCTTCCACCGTGCTACATCATGTCCTG
PLK-PBD-R	GTTACGTCGACTCCCCTCCCTGACCGAGCTGCCT
Mopholino sequences	
Control	CCTCTTACCTCAGTTACAATTTATA
Anti-*glplk*	AGCTCCCACCGCAAAAGCCAAAATT
Real-time PCR	
PLK-RT-F (GL50803_104150)	GTCACGTTTATGAGCGAGAA
PLK-RT-R (GL50803_104150)	CTATTCCCCTCCCTGACCGA
Actin-F (GL50803_15113)	GTCCGTCATACCATCTGTTC
Actin-R (GL50803_15113)	GTTTCCTCCATACCACACG
Kinase assay	
PLK-GBK-F	GCACGAATTCATGTCCCACAGCAACGCCCCAGAA
PLK-GBK-R	CTACAGCGGCCGCCTATTCCCCTCCCTGACCGAGCT
GlPLK phosphorylated residue mutant	
PLKT183A-F	TGGGCCATGTGTGGAGCGCCAAACTTT
PLKT183A-R	GAGAAAGTTTGGCGCTCCACACAT
Recombinant protein for antibodies	
rGlGAP1-F	GATTGAATTCATGCCTATTCGCCTCGGAAT
rGlGAP1-R	GCCTAGCGGCCGCGGCAGCCCTTGGACCCGACGTA
rGlCENH3-F	GATCCATATGATGAGCGGAGGCTCACGG
rGlCENH3-R	TACCGTCGACCCGTAGTGAATTTAAGTT

[a] Restriction enzyme sites are underlined.

[b] Mutated bases are indicated as italic letters.

Twenty micrograms of pGlPLK.pac were transfected into 1×10^7 *Giardia* trophozoites by electroporation under the following conditions: 350 V, 1000 μF, and 700 Ω (Bio-Rad, Hercules, CA, USA). Expression of HA-tagged GlPLK was confirmed by western blotting. *Giardia* trophozoites carrying pΔ.pac [17] were included as a control.

Two truncated GlPLK proteins were also ectopically expressed in *Giardia* trophozoites. A 1,293-bp DNA fragment encoding the N-terminal portion of GlPLK (KD + linker region) was amplified using the primers Pplk-F and PLK-NL-R (Table 1) and then cloned into *Not*I and *Hind*III sites of pKS-3HA.neo to generate pGlPLKKDL.neo. To express the two PBDs of GlPLK, a 150-bp *glplk* promoter region (amplified by PCR using primers Pplk-F and Pplk-R) was cloned into pKS-3HA.neo, to produce the pPplk-3HA.neo plasmid. Subsequently, DNA encoding the PBDs of G1PLK was amplified using PLK-PBD-F and PLK-PBD-R primers and then cloned into the *Hind*III and *Sal*I regions of pPplk-3HA.neo to obtain pGlPLKPBD.neo. These plasmids were transfected into *Giardia* trophozoites as described above. The expression of these truncated proteins was examined by western blotting using anti-HA antibodies

Western blotting

Extracts prepared from *Giardia* cells carrying pΔ.pac or pGlPLKHA.pac were separated via sodium dodecyl sulfate-polyacrylamide gel electrophoresis (SDS-PAGE) and transferred onto a polyvinylidene fluoride membrane (Millipore, Bedford, MA, USA). The membrane was incubated with monoclonal mouse anti-HA antibodies (1:1,000; Sigma-Aldrich) in a TBST solution (Tris-buffered saline with Tween 20; 50 mM Tris-HCl, 5% skim milk and 0.05% Tween 20) at 4 °C overnight. Then the membranes were incubated with horseradish peroxidase-conjugated secondary antibodies, following which immunoreactive proteins were visualized using an Enhanced Chemiluminescence System (Thermo Fisher Scientific, Waltham, MA, USA). Membranes were incubated in a stripping buffer (Thermo Fisher Scientific) at room temperature for 20 min and then reacted with polyclonal rat antibodies against protein disulfide isomerase 1 (PDI1; GL50803_29487) of *G. lamblia* (1:10,000) as the loading control [17].

Immunofluorescence assay (IFA)

Giardia cells were attached on glass slides coated with L-lysine for 10 min and then fixed with chilled methanol for 5 min followed by PBS/0.5% Triton X-100 for 10 min. After blocking for 1 h in PBS/5% goat serum/3% bovine serum albumin, the cells were incubated with primary antibodies overnight at 4 °C and subsequently treated with fluorescent dye-conjugated secondary antibodies. The samples were mounted with VECTASHIELD Anti-fade Mounting Medium with DAPI (Vector Laboratories) and then examined with an Axiovert 200 fluorescent microscope (Carl Zeiss).

The following antibodies were used at the indicated dilution: anti-HA mouse monoclonal antibodies (1:100; Sigma-Aldrich), anti-HA rat monoclonal antibodies (1:100; Roche Applied Science, Mannheim, Germany), anti-α-tubulin mouse antibodies (1:800; Sigma-Aldrich), anti-GlCentrin rat antibodies (1: 100; Kim and Park, 2019), Alexa Fluor 488-conjugated goat anti-mouse IgG (1:100; Molecular Probes, Waltham, MA, USA), Alexa Fluor 488-conjugated goat anti-rat IgG (1:400; Molecular Probes), Alexa Fluor 555-conjugated anti-rat IgG (1:100; Molecular Probes), and Alexa Fluor 568-conjugated anti-mouse IgG (1:100; Molecular Probes).

The antibodies specific to the phosphorylated form of PLK were purchased from Abcam (ab39068; Cambridge, MA, USA) used for IFA of *G. lamblia* cells (1:100) along with anti-HA antibodies to discern the localization of phosphorylated GlPLK.

Morpholino knockdown

GlPLK expression was knocked down using morpholino, as described [18]. Specific morpholino for GlPLK was designed by Gene Tools, and their sequences are listed in Table 1. Non-specific oligomers were used as a control morpholino (Table 1). Cells (5×10^6 in 0.3 mL medium) were treated with the lyophilized morpholino at a final concentration of 100 μM. After electroporation, the cells were grown for 24 or 48 h and then analyzed for GlPLK expression by western blotting.

Cell cycle synchronization in G. lamblia **using nocodazole and aphidicolin**

Giardia trophozoites (5×10^5 cells/mL) were incubated in a modified TYI-S-33 medium to 60% confluency. A portion of these cells was treated with 100 nM nocodazole (Sigma-Aldrich) for 2 h and harvested as G2/M-phase cells. The remaining nocodazole-treated cells were treated with 6 μM aphidicolin (Sigma-Aldrich) for 6 h to obtain G1/S-phase cells. As a control, *Giardia* trophozoites were treated with 0.05% DMSO instead of nocodazole and aphidicolin.

These cells were then analyzed by flow cytometry to determine the ploidy of their DNA. Intracellular levels of GlPLK protein in the DMSO-treated, nocodazole-treated, and nocodazole/aphidicolin-treated *Giardia* cells were determined by western blotting. In addition, intracellular levels of *glplk* transcripts were measured in these cells.

Quantitative real-time PCR

Total RNA was prepared from G1/S-phase and G2/M-phase cells using TRIzol (Invitrogen, Carlsbad, CA, USA) according to the manufacturer's instructions. Five micrograms of RNA were converted into complementary DNA (cDNA) using an Improm-II Reverse Transcription System (Promega, Madison, WI, USA). Real-time PCR was performed using a LightCycler System and LightCycler 480 SYBR Green I Master Kit (Roche Applied Science). The conditions for real-time PCR were as follows: pre-incubation at 95 °C for 5 min followed by 45 amplification cycles of 94 °C for 1 min, 56 °C for 1 min, and 72 °C for 1 min. The nucleotide sequences of the forward and reverse primers used for real-time PCR are listed in Table 1. The *G. lamblia* actin-related gene (*glactin*; GL50803_15113) transcript was used to normalize the amount of mRNA in the samples.

Subcellular protein fractionation

Various *G. lamblia* cells (interphase, G1/S-phase, and G2/M-phase cells; 2×10^9 cells) were lysed in hypotonic buffer (10 mM HEPES-KOH, 10 mM KCl, 1.5 mM $MgCl_2$, 0.2 mM PEFA1023 pH 7.9, 0.5% Nonidet P-40, 20 mM NEM, and protease inhibitor cocktail), as described previously [19]. After a 10 min-centrifugation at 16,000 × *g*, supernatants were collected as cytoplasmic extracts. The pellets were treated with high-salt buffer (450 mM NaCl, 50 mM Tris-HCl, 2 mM DTT, 1% NP-40, 20 mM NEM, and protease inhibitor cocktail) for 10 min and then centrifuged at 4 °C for 15 min at 16,000 × *g*. The supernatants were collected as nuclear extracts. Equal amounts of cytoplasmic and nuclear extracts were analyzed by western blotting using anti-HA (1:1,000), anti-GlGAP1 (GI50803_6687; 1:10,000), or anti-GlCENH3 antibodies (GL50803_20037; 1:5,000).

Formation of anti-GlGAP and anti-GlCENH3 antibodies

A 1,011-bp DNA fragment encoding GlGAP1 or a 471-bp DNA fragment encoding GlCENH3 were amplified from the *Giardia* genome. Each fragment was cloned into pGEX4T-1 or pET21b to produce pGEX-GlGAP1 or pET-GlCENH3, respectively (Table 2). GST-GlGAP1 and HA-tagged GlCENH3 were overexpressed in *E. coli* BL21 (DE3) with the addition of 1 mM IPTG at 37 °C. The resultant recombinant proteins were excised from the SDS-PAGE gel and used to immunize Sprague-Dawley rats (2-week-old, female) to produce polyclonal antibodies, as previously described [21]. All primers used are listed in Table 1.

Table 2
Strains and plasmids used in this study

Organism/ Plasmid	Description[a]	Source/ Reference
Giardia lamblia		
ATCC 30957	Clinical isolate	ATCC
Escherichia coli		
DH5α	*supE44, ΔlacU169* (*Φ80 lacZ ΔM15*), *hsdR17, recA1, endA1, gyrA96, thi-1, relA1*	Invitrogen
BL21 (DE3)	*F', ompT, hsdSB*(rB^-mB^-) *gal, dcm* (*DE3*)	Invitrogen
Plasmids		
pGFP.pac	Shuttle vector, Amp^R, *pac* gene	Singer et al., 1998 [16]
pΔ.pac	*gfp* gene deletion	Kim and Park, 2019 [17]
pGlPLK.pac	pGFP.pac, 2137-bp encoding *glplk* (GiardiaDB ID GL50803_104150)	This study
pKS-3HA.neo	Shuttle vector, Amp^R, *neo* gene	Gourguechon and Cande, 2011 [20]
pGlPLKKDL.neo	pKS-3HA.neo, 1293-bp encoding kinase domain and linker of *glplk*	This study
pPplk-3HA.neo	pKS-3HA.neo, 150-bp encoding promoter region of *glplk*	This study
pGlPLKPBD.neo	pKS-3HA.neo, 894-bp encoding promoter region and PBDs of *glplk*	This study
pGlPLKK51R.neo	pKS-3HA.neo, 2137-bp encoding K51R *glplk*	This study
pGlPLKT179A.neo	pKS-3HA.neo, 2137-bp encoding T179A *glplk*	This study
pGlPLKT183A.neo	pKS-3HA.neo, 2137-bp encoding T183A *glplk*	This study
pGlPLKT179AT183A.neo	pKS-3HA.neo, 2137-bp encoding T179AT183A *glplk*	This study
pGBKT7	$Gal4p_{(1-147)}$ DNA-BD, TRP1, Kan^R, c-Myc Epitope	Clontech
pGBK-GlPLK	pGBKT7, 2137-bp encoding *glplk*	This study
pGBK-GlPLKK51R	pGBKT7, 2137-bp encoding K51R *glplk*	This study
pGBK-GlPLKT179A	pGBKT7, 2137-bp encoding T179A *glplk*	This study
pGBK-GlPLKT183A	pGBKT7, 2137-bp encoding T183A *glplk*	This study
pGBK-GlPLKT179AT183A	pGBKT7, 2137-bp encoding T179AT183A *glplk*	This study
pGEX4T-1	Expression vector, Amp^R, GST	GE Healthcare
pGEX-GlGAP1	pGEX4T-1, 1011-bp encoding *glgap1*	This study
pET21b	Expression vector, Amp^R	Novagen
pET-GlCENH3	pET21b, 471-bp encoding *glcenh3*	This study

[a] Amp, ampicillin; Kan, kanamycin; R, resistant; DNA-BD, DNA binding domain; AD-activation domain; HA, hemagglutinin

Immunoprecipitation (IP)

G. lamblia trophozoites (2×10^9 cells) were washed three times with ice-cold PBS before being lysed in protein lysis buffer (10 mM Tris•Cl, 5 mM EDTA, 130 mM NaCl, and 1% Triton X-100, pH 7.4) containing protease inhibitor cocktail. Lysates were pre-cleared by adding Pierce Protein A/G Agarose (Thermo Fisher Scientific) for 1 h at 4 °C with end-over-end rotation. Subsequently, pre-washed lysates were reacted with monoclonal mouse anti-HA-agarose antibodies produced in mouse (Sigma-Aldrich) at 4 °C overnight. Beads were washed 3 times, and twice for 10 min in IP washing buffer (50 mM Tris•Cl, 150 mM NaCl, and 1% Triton X-100, pH 7.4). After re-suspending in 1 × SDS sample buffer, the precipitates were analyzed by western blotting using anti-HA antibodies.

In vitro **transcription/translation synthesis of rGlPLK proteins**

The TNT T7 Coupled Reticulocyte Lysate System (Promega) was used for the *in vitro* synthesis of c-Myc-tagged GlPLK. The DNA template (0.5 μg) was incubated with the transcription/translation mix in a total volume of 50 μL at 30 °C for 90 min. The synthesized protein products were analyzed by SDS-PAGE and visualized by western blotting.

Kinase assay

Both IP extracts and rGlPLK proteins, which were prepared as mentioned above, were resuspended in 20 μL kinase buffer (50 mM Tris-HCl, 10% glycerol, 5 mM $MgCl_2$, 150 mM NaCl, 50 mM KCl, and 1 mM DTT, pH 8.0), and then used for kinase assays in the presence of 2.5 μCi [γ-^{32}P]ATP (3000 Ci/mmol; PerkinElmer, Waltham, MA, USA). The kinase reactions were processed for 30 min at 30 °C and then stopped by adding SDS loading buffer. Samples were separated on 12% SDS-PAGE gels, which were then dried and subjected to autoradiography.

Generation of mutant GlPLK proteins by site-directed mutagenesis

As candidate sites for phosphorylation, Lys51 was modified to Arg, whereas Thr179 and Thr183 were mutated to Ala. The following plasmids were supplied by Macrogen for *in vitro* synthesis of rGlPLK and *in vivo* expression of GlPLK in *Giardia*: pGBK-GlPLKK51R, pGBK-GlPLKT179A, pGBK-GlPLKT183A (for *in vitro* synthesis), pGlPLK51R.neo, pGlPLKT179A.neo, and pGlPLKT184A.neo (for expression in *Giardia*). Plasmids for mutant rGlPLKT179AT183A were generated by site-directed mutagenesis using primers carrying the substitution. To generate a plasmid for expression of the T179AT183A double mutant in *Giardia*, two DNA fragments were amplified using the pGlPLKT179A.neo plasmid as a template with two primer sets, Pplk-F/PLKT183A-R or PLKT183A-F/PLK-PBD-R. The resulting PCR products were used as templates for a second round of PCR with the primers Pplk-F and PLK-PBD-R. The DNA fragment was then cloned into the pKS-3HA.neo, resulting in the pGlPLKT179AT183A.neo plasmid. The plasmid for *in vitro* synthesis of T179AT183A double mutant rGlPLK was constructed in the same manner. Briefly, two PCR fragments were amplified using PLK-GBK-F/PLKT183A-R or PLKT183A-F/PLK-GBK-R. Using these DNA fragments as templates, a second round of PCR was performed with the primers PLK-GBK-F and PLK-GBK-R to obtain the pGBK-PLKT179AT183A plasmid.

Statistical analysis

Data are presented as the mean ± standard deviation from three independent experiments. Statistical analyses for pair-wise comparisons were performed using Student's *t*-tests to evaluate the statistical significance of these results. Differences with *P*-vlaues of less than 0.05 were considered significant. Data with *P*-values of less than 0.01 are indicated with two asterisks, whereas data with *P*-values between 0.01 and 0.05 are indicated with a single asterisk.

Results

Inhibition of PLK activity affects the cell cycle and flagella biogenesis in G. lamblia

In order to define the role of PLK, *G. lamblia* trophozoites were treated with various concentration of GW843682X (GW), an ATP-competitive inhibitor of PLK1 and PLK3 (Additional file 1: Figure S1a). The growth of *G. lamblia* was inhibited proportionally to the GW concentration, and the 50% inhibitory concentration for cell death (IC_{50}) was 5 μM. Control cells, i.e. *Giardia* trophozoites treated with 0.05% dimethyl sulfoxide (DMSO), were found to be a mixture of G1/S-, and G2/M-phase cells, and the cells at G2/M-phase were dominant (72%), as reported previously (Additional file 1: Figure S1b) (Poxleitner et al., 2008). Flow cytometry of the DNA content of the 5 μM GW-treated cells also demonstrated that more cells were present at the G1/S-phase (up to 70%) than that in untreated cells (16%), whereas the percentages of G1/S-phase cells decreased proportionally to GW concentration (Additional file 1: Figure S1b). These results indicated that the inhibition of PLK in *Giardia* causes cell cycle arrest, eventually leading to growth inhibition of *Giardia* trophozoites.

To determine the effect of PLK inhibition on *Giardia* division, 5 μM GW-treated cells were observed by DAPI staining (Fig. 1a). As a result, the nuclei of most cells appeared larger than those of DMSO-treated cells. The percentage of cells with four nuclei was significantly increased to 6.3% (from 1.6% of the control cells; $P = 0.0018$), indicating that GW induced cell cycle arrest at cytokinesis. These cytokinesis-defective *Giardia* cells were further classified into the following four sequential phenotypes: disorganized cells impertinent for cytokinesis, cells defective in furrow formation, arrested cells at cytokinesis, and cells failed at abscission step (Fig. 1b). The percentages of cells showing disorganization were increased to 18% from 9% (control) ($P = 0.0018$). On the contrary, the percentages of *Giardia* cells defective in the subsequent three steps were not significantly affected by GW-treatment.

To observe the morphology of PLK-inhibited *Giardia* trophozoites, 5 μM GW-treated cells were stained with Giemsa. Interestingly, GW treatment was found to trigger the formation of *Giardia* trophozoites with longer flagella (Fig. 1c). The extension of flagella in the GW-treated cells was documented by quantitatively measuring caudal flagella length. These data clearly showed that GW-treated cells had longer caudal flagella (8.6 μm) than the untreated cells (5.4 μm) ($P = 0.0023$).

Localization of GlPLK and definition of domains required for its localization in Giardia trophozoites

A homology search in the *Giardia* database indicated an ORF (GL50803_104150), as a putative *G. lamblia* PLK, GlPLK. Amino acid sequences deduced from the ORF were aligned with those of human and *Trypanosoma brucei* PLKs, and PLKs were deduced from the nucleotide sequences (GenBank accession number NP_005021.2 and *Trypanosoma* database ORF number Tb927.7.6310, respectively), showing 31–34% identity (Additional file 2: Figure S2). The ORF was postulated to encode a protein of pI = 8.8, and a search of domains within this ORF using the Entrez program (http://www.expasy.org/) indicated that it does contain a serine-threonine kinase domain (KD) at the amino-terminal portion (from amino acid residue No. 20 to 309). In addition, a block of amino acids near the carboxyl terminus was proposed as PBDs (from amino acid residue No. 432 to 517 and 563 to 640), which had been conserved in diverse PLKs [22]. Based on the alignment of GlPLK with other PLKs, Lys51 was suggested as a residue that initially receives phosphate from ATP, and Thr179 and Thr183 residues were proposed as target sites that are subsequently phosphorylated.

A plasmid, pGlPLK.pac, was prepared (Fig. 2a) and used to construct transgenic *Giardia* trophozoites expressing HA-tagged GlPLK. Western blotting of the resulting *G. lamblia* extracts confirmed the expression of HA-tagged GlPLK as an immunoreactive band with a molecular weight of 75 kDa (Fig. 2b). In contrast, the extracts of *G. lamblia* carrying the vector control, pΔ.pac, did not produce any immunoreactive bands in the same analysis. Western blotting of the same membrane with anti-GlPDI1 antibodies [17] served as a loading control for the total amount of protein in the extracts used for this assay.

The localization of GlPLK was determined using *Giardia* expressing HA-tagged GlPLK (Fig. 2c). In *Giardia*, GlPLK was found in basal bodies and axonemes at the interphase. Localization at basal bodies was maintained in the dividing cells, i.e., cells at metaphase, anaphase, and telophase as well as cytokinesis. In

cells at anaphase and telophase, GlPLK was also present in mitotic spindles and possibly in the midbody between two daughter cells.

To confirm the localization of GlPLK, *Giardia* cells expressing HA-tagged GlPLK were double-stained for GlPLK and microtubules (MTs) using anti-HA and anti-α-tubulin antibodies, respectively (Additional file 3: Figure S3a). In *Giardia* cells at interphase as well as during division, GlPLK was found together with MTs in the basal bodies and axonemes. In addition, *Giardia* cells during cell division demonstrated co-localization of GlPLK with MTs in the mitotic spindles present between two separated groups of basal bodies.

Basal bodies serve as the MT-organizing center (MTOC) in *G. lamblia* [23], which can be observed by staining for its marker, centrin. Additional immunofluorescence assays (IFAs) for *Giardia* expressing HA-tagged GlPLK were performed using antibodies against HA and *G. lamblia* centrin (GlCentrin) (Additional file 3: Figure S3b). These double-stained *Giardia* cells clearly showed co-localization of GlPLK and GlCentrin during cell division as well as at interphase.

As mentioned above, GlPLK comprises two regions, containing a KD and two PBDs (Additional file 4: Figure S4a). The region between KD and PBDs was named linker. To examine whether KD and/or PBD play a role in GlPLK localization, two plasmids were constructed, i.e., pGlPLKKDL.neo and pGlPLKPBD.neo (expression of the KD-linker and PBDs of GlPLK, respectively). The truncated GlPLK proteins, KD-linker and PBDs, were observed in the form of immunoreactive bands with a molecular weight of 60 and 40 kDa, respectively, by western blotting using anti-HA antibodies (Additional file 4: Figure S4b).

G. lamblia cells carrying pGlPLKKDL.neo or pGlPLKPBD.neo were double-stained with anti-HA and anti-α-tubulin antibodies (Additional file 4: Figure S4c, d) or anti-HA and anti-GlCentrin antibodies (Additional file 4: Figure S4e, f) in order to observe whether these truncated GlPLKs were correctly localized in mitotic spindles and basal bodies. Both the truncated GlPLK proteins were present in the basal bodies, as was the full-length GlPLK. However, both proteins showed defective localization in the mitotic spindles during cell division. These results suggested that both KD and PBD are required for GlPLK localization in mitotic spindles during *Giardia* cell division.

Effect of GlPLK knockdown on cell division and flagella biogenesis in G. lamblia

To define the role of this putative GlPLK in *G. lamblia*, we designed an anti-*glplk* morpholino to block the translation of *glplk* mRNAs (Table 1). A control morpholino (non-specific oligomers) was also synthesized and transfected into *G. lamblia* trophozoites by electroporation (Table 1). These extracts were examined to determine their intracellular GlPLK levels at 24 h post-transfection by western blotting using anti-GlPLK antibodies (Fig. 3a). In cells treated with anti-*glplk* morpholino, the amount of GlPLK at 24 h post-transfection had decreased to 37% of that in cells treated with control morpholino ($P = 0.011$).

The effect of GlPLK knockdown on cell division was determined based on the mitotic index, which showed that the proportion of cells with four nuclei increased from 2% in control-morpholino-treated cells to 8% in cells treated with anti-*glplk* morpholinos (Fig. 3b; $P = 0.0024$). The second assay was used to distinguish between *Giardia* at the different stages of cytokinesis (i.e., disorganized, no furrow, cytokinesis, and abscission) (Fig. 3c). The percentage of disorganized cells was significantly increased in GlPLK-knockdown cells (14% compared to 9% of control cells; $P = 0.019$). However, cell numbers at the subsequent steps were not affected by anti-*glplk* morpholino. GlPLK depletion also resulted in the formation of *Giardia* trophozoites with longer flagella (Fig. 3d). The length of caudal flagella in cells treated with anti-*glplk* morpholino was increased to 8.1 μm compared to 5.2 μm in the untreated cells ($P = 0.0006$). As the phenotypes of cells with morpholino-mediated depletion of the putative *glplk* gene and of GW-treated cells coincided, these results clearly demonstrated that this putative ORF encodes PLK in *G. lamblia*.

Expression pattern of GlPLK at G1/S- and G2/M-phase of the Giardia cell cycle

As human PLK1 is highly expressed during mitosis [24], we examined whether the expression of GlPLK varies in a cell phase-dependent manner. *Giardia* cells were treated with nocodazole to prepare G2/M-phase cells or sequentially with nocodazole and aphidicolin to acquire G1/S-arrested cells. The stage of the resulting *Giardia* cells carrying pGlPLK.pac was confirmed by flow cytometry (Additional file 5: Figure S5a). Control cells, i.e. *Giardia* trophozoites treated with 0.05% DMSO, were found to be a mixture of G1/S-, and G2/M-phase cells, and the cells at G2/M-phase were dominant (76%).

Western blotting of these extracts using anti-HA antibodies demonstrated a constant amount of GlPLK in G2/M- and G1/S-phase cells as well as interphase cells (Additional file 5: Figure S5b). The immunoreactive band was absent from the extracts prepared from *Giardia* carrying pΔ.pac. Western blotting of the same blot using anti-GlPDI1 antibodies served as a loading control.

Constitutive expression of GlPLK was also examined using an alternative method, quantitative RT-PCR (Additional file 5: Figure S5c). The relative level of *glplk* transcripts to *glactin* transcripts remained constant (60–64%) in G1/S-, G2/M-phase, and interphase cells.

Localization of GlPLK into nucleus of G. lamblia

In order to function properly during mitosis, PLK1 should be localized into specific sites through differential interaction with various scaffold proteins [22]. The nucleus is the one of the subcellular locations where PLK1 localizes at G2 phase [25]. Therefore, we investigated whether GlPLK exists in the nuclei of *Giardia* trophozoites. *Giardia* extracts were prepared from *Giardia* cells expressing HA-tagged GlPLK, and then further divided into cytoplasmic and nuclear fractions. These extracts were analyzed by western blotting using anti-HA antibodies (Fig. 4a). In addition, extracts were evaluated for *G. lamblia* glyceraldehyde 3-phosphate dehydrogenase (GI50803_6687; GlGAP1) and *G. lamblia* centromeric histone H3 (GL50803_20037; GlCENH3) as a marker for cytoplasmic and nuclear proteins, respectively. GlPLK was found in both cytoplasmic and nuclear fractions. As expected, GlGAP1 was mainly present in the cytoplasmic fraction, and GlCENH3 was found only in the nuclear fraction.

Giardia cells at G1/S-phase and G2/M-phase were prepared and analyzed for nuclear localization of GlPLK (Fig. 4b). Both G1/S- and G2/M-phase cells demonstrated GlPLK localization in the nuclei and more GlPLK was found in the nuclear fraction of G2/M-phase cells than in that of G1/S-phase cells.

GlGAP1 was present in the cytoplasmic fraction of all examined phases, whereas GlCENH3 was found in the nuclear fraction of the G1/S-phase and G2/M-phase cells.

Localization of phosphorylated GlPLK in G. lamblia

Constitutive expression of GlPLK (Additional file 5: Figure S5b, c) suggests that the activity of GlPLK may be regulated by its activation status, possibly by phosphorylation. *Giardia* trophozoites were double-stained with anti-HA and anti-phospho-PLK antibodies against phosphorylated T210 of human PLK1 (Additional file 6: Figure S6). Both anti-HA and anti-phospho-PLK antibodies stained the basal bodies in both interphase and dividing cells. In dividing cells, phospho-GlPLK was found at mitotic spindles, where localization was limited to the middle region, whereas HA-tagged GlPLK was more widely present in the mitotic spindles of the dividing cells.

In vitro **auto-phosphorylation of GlPLK and identification of critical amino acid residues for its auto-phosphorylation**

The putative amino acid sequence of GlPLK indicates a serine-threonine KD at the amino terminus and two PBDs at the carboxyl terminus (Fig. 5a). Based on comparison with other PLKs, it was predicted that Lys51 is the primary binding site for ATP, and that the phosphate of Lys51 is eventually transferred to Thr179 and Thr183 in the activation loop.

Immunoprecipitated (IP) extracts were prepared from *Giardia* expressing HA-tagging GlPLK. These GlPLK IP extracts were reacted with [γ-^{32}P]ATP to radiolabel the protein (75 kDa) (Fig. 5b). Control IP extracts were prepared in the same manner by incubating *Giardia* extracts with mouse preimmune serum instead of anti-HA antibodies. Incubation of the control IP extracts with [γ-^{32}P]ATP did not result in the labeling of GlPLK.

Kinase assays were also performed using recombinant GlPLK (rGlPLK), which was synthesized using *in vitro* transcription and translation systems (Fig. 5c). Upon incubation with [γ-^{32}P]ATP, rGlPLK was radiolabeled due to auto-phosphorylation.

To define the amino acid residues that are critical for the auto-phosphorylation of GlPLK, several recombinant GlPLK proteins were also synthesized using *in vitro* transcription/translation systems and used for kinase assays (Fig. 5d). Specifically, the two putative phosphorylation sites were mutated to Ala, and the resulting mutant GlPLK proteins (GlPLKT179A and GlPLKT183A) were used for kinase assays. In an additional mutant GlPLK, the putative ATP binding site of Lys51 was mutated to Arg (GlPLKK51R). Both GlPLKT179A and GlPLKT183A proteins were auto-phosphorylated, although the efficiency of auto-phosphorylation was lower than that of wild-type GlPLK. When both Thr179 and Thr183 were mutated to Ala in GlPLK, the resulting protein exhibited a dramatic decrease in its ability for auto-phosphorylation. Conversion of Lys51 to Arg abolished the auto-phosphorylation of rGlPLK. This result demonstrated that both Thr179 and Thr183 in the activation loop of GlPLK were phosphorylated. As expected, Lys51 of GlPLK was confirmed to serve as an ATP binding site.

Role of GlPLK phosphorylation in cytokinesis and flagella biogenesis in G. lamblia

The subsequent experiments were performed to define the physiological roles of GlPLK. Transgenic *G. lamblia* carrying pGlPLKK51R.neo was constructed. In addition, *Giardia* cells ectopically expressing mutant PLK (T179AT183A) were prepared. Western blotting demonstrated that the transgenic cells expressed HA-tagged GlPLK proteins (data not shown).

The growth of various *Giardia* cells (ectopically expressing GlPLK, mutant GLPLKK51R, mutant GlPLKT178AT183A, or carrying vector control) was determined (Fig. 6a). The growth of *Giardia* cells overexpressing wild-type GlPLK was similar to that of the control cells. However, *Giardia* cells expressing mutant GlPLKs showed inhibited growth as compared with those expressing wild-type GlPLK.

These cells were then used to evaluate mitotic indices by determining the percentages of cells with four nuclei (Fig. 6b). The percentage of cells with four nuclei was increased to 6.7% in transgenic *G. lamblia* expressing mutant GlPLKK51R compared with that in cells transfected with the vector control (1.7%) or GlPLK-expressing plasmid (1.4%) ($P = 0.003$). *G. lamblia* ectopically expressing mutant GlPLKT179AT183A also showed arrest at cytokinesis (7.3%) ($P = 0.010$). These results indicate that Lys51 as well as two Thr residues (Thr179 and Thr183) in GlPLK may play a role in cell division in *Giardia*. In addition, ectopic expression of these mutant GlPLK resulted in the extension of the length of caudal flagella from 5% (vector and wild-type GlPLK) to 8-8.2% (mutant GlPLK) (Fig. 6c). These data indicated that GlPLK plays a role in regulating the cell cycle in *Giardia*, and that the phosphorylation of GlPLK is critical for its *in vivo* function.

Discussion

Mammalian PLK is a multi-faceted kinase that controls several steps of the cell cycle [26]. In contrast to the presence of PLK paralogues in other systems, *G. lamblia* seems to have one PLK, the function of which was demonstrated herein with a PLK chemical (Fig. 1, Additional file 1: Figure S1) and anti-*glplk* morpholino (Fig. 3).

These experiments provide evidence for the role of GlPLK in cytokinesis and flagella biogenesis, but not in other aspects of the cell cycle, such as centrosome maturation, kinetochore formation, and mitotic spindle function. Inhibition of GlPLK using GW or anti-*glplk* morpholino affected the early stage of cytokinesis, as shown by an increased number of disorganized cells, which suggests its role in chromosome segregation. However, GlPLK localization at basal bodies, which serves as an MTOC in *Giardia*, as well as mitotic spindles and the midbody for dividing cells, indicate that GlPLK plays an important role in mitosis as mammalian PLK1 [22], which is further strengthened by IFAs using anti-phospho PLK antibodies (Additional file 6: Figure S6). Moreover, GlPLK localization at basal bodies and mitotic spindles was confirmed by co-localization experiments using marker proteins (Additional file 3: Fig. 3a, b). The plausible localization of GlPLK at the midbody of dividing cells should be confirmed by developing marker protein(s) for this region (Fig. 2, Additional file 6: Figure S6). Interestingly,

Giardia trophozoites were arrested at G1/S-phase upon GW treatment (Additional file 1: Figure S1b), suggesting that GlPLK also plays a role in this phase. In contrast to the restricted functions of PLK2, PLK3, and PLK5 in non-proliferating vertebrate cells [27], PLK1 and PLK4 are highly conserved. PLK1 is a multi-functional kinase involved in mitosis and cytokinesis, whereas PLK4 is known as a centriole assembly factor in S-phase [28]. It is possible that GlPLK functions as a combined form of PLK1/PlK4. However, the unavailability of tools for analyzing the cell cycle and the short time required for the cytokinesis of *Giardia* trophozoites [6] hamper direct analysis of the *Giardia* cell cycle.

Since subcellular localization of PLK occurs via interactions with various scaffold proteins and is important in its functions in other systems [29], we investigated whether GlPLK is localized in the nuclei of *Giardia* trophozoites (Fig. 4). Most notably, IFAs showed no evidence of nuclear localization of GlPLK (Fig. 2, Additional file 3: Figure S3, Additional file 6: Figure S6). However, the subcellular fractionation assay showed that GlPLK is present in nuclear fractions, similar to the nuclear protein marker centromeric histone H3 (Fig. 4a), and the amount of GlPLK increased at G2/M-phase compared to that at G1/S-phase (Fig. 4b). The nuclear localization signal (NLS) and destruction box (D-box) were not observed in the amino acid sequence of GlPLK, whereas PLK1 has canonical sequences for NLS and D-box [30]. Based on studies showing that PLK1 SUMOylation is involved in its nuclear localization [31, 32], a putative SUMO interaction sequence and a target sequence for SUMO were found in GlPLK using a SUMOylation prediction program (GPS SUMP 1.0). The absence of D-box in cyclin B, AK, and PLK of *G. lamblia* indicates a regulatory mechanism other than ubiquitin-mediated degradation [33]. Therefore, it will be interesting to study how the SUMOylation of GlPLK affects its localization and function during the cell cycle of *G. lamblia*.

In mammalian systems, PLK1 interacts with other proteins via its PBDs, and these interactions are critical for the spatial and temporal function of PLKs as they control their subcellular localization [34]. The role of KD and PBD in the localization of GlPLK were examined using *Giardia* ectopically expressing truncated GlPLK (Additional file 4: Figure S4c-f). The absence of KD or PBD affect localization differently at basal bodies than that at mitotic spindles. Although technical limitations cannot be ruled out, this difference may be due to different requirements of the target protein(s) for being localized at specific positions.

In human, the level of PLK1 is at its peak at metaphase [24]. A study using counterflow centrifugal elutriation of *Giardia* cells revealed a two-fold increase in *glplk* gene expression at G2/M-phase gene showing two-fold increase [5]. However, real-time PCR and western blotting for GlPLK expression did not show any difference based on the phase of the cell cycle (Additional file 5: Figure S5b, c). This discrepancy may be due to the method used to prepare phase-enriched *Giardia* cells, which were synchronized using chemicals in our study.

Auto-phosphorylation of GlPLK has been demonstrated *in vitro* via two different methods, i.e., using *Giardia* extracts IP with anti-HA antibodies or with rGlPLK synthesized *in vitro* (Fig. 5b-d). Mutagenesis of GlPLK and kinase assays using the mutant rGlPLKs confirmed that Lys51 is a critical residue that receives the phosphate from ATP. Two putative phosphorylation residues, Thr179 and Thr183, play a complementary and redundant role, because phosphorylation is dramatically affected only when both of the residues are mutated.

The situations are more complex *in vivo*, as phosphorylation of PLK1 can occur in spatial and temporal modes. This phosphorylation depends upon the correct localization into the site at which the target protein is present and on the binding of the target proteins to the PBD of PLK1 [35]. When mammalian PLK1 is phosphorylated by AKA, mitosis is initiated in the cells [36]. In addition, cyclin B-CDK1-dependent phosphorylation of aurora borealis is a pre-requisite for PLK activation [37]. GlAK was found in basal bodies (in interphase and dividing cells) and mitotic spindles (in dividing cells), and AK inhibition resulted in a cytokinesis defect [23, 38, 39]. These results suggested that GlPLK may function together with GlAK during the cell cycle of *G. lamblia*. Moreover, an interaction between these two kinases was observed via co-immunoprecipitation (Kim et al., unpublished result).

The role of GlPLK was further confirmed by ectopically expressing mutant GlPLK in *Giardia* trophozoites (Fig. 6). In addition to cytokinesis, expression of mutant GlPLK proteins (K51R, and T179AT183A) inhibited the growth of *Giardia* trophozoites, indicating that GlPLK affects cell division in *Giardia*. However, expression of wild-type GlPLK did not affect cell growth and cytokinesis in *G. lamblia*. This result demonstrated that the amino acid residues critical for GlPLK phosphorylation are also important for GlPLK function *in vivo*.

Lastly, we wish to address the effect of the GlPLK defect on flagella length (Fig. 1c, Fig. 3d, Fig. 6c). Both GW-mediated and morpholino-mediated inhibition of GlPLK resulted in the extension of caudal flagella in *Giardia.* Localization of GlPLK at basal bodies, which function as an MTOC, indicated that GlPLK might play a role in MT nucleation. A previous study demonstrated that depletion of the γ-tubulin ring complex (γ-TuSC) affects MT nucleation, resulting in shortening of the flagella [17]. Overexpression of dominant-negative mutant kinesin-13, a motor protein, produced *Giardia* with longer flagella and defective mitotic spindles [40]. Taken together, these data suggest that GlPLK modulates flagella biogenesis via interaction and/or modification of these proteins.

Conclusions

In this study, we demonstrated that *G. lamblia* has one PLK, which functions in the cell cycle and flagella formation, as revealed by inhibitor-mediated and morpholino-mediated inhibition. We also demonstrated that the phosphorylation of GlPLK also plays an important role in cell growth, cytokinesis and flagella biogenesis in *Giardia*.

Abbreviations

PLK: polo-like kinase; GW: PLK-specific inhibitor GW843286X; AK: aurora kinase; CDK1: cyclin-dependent kinase1; KD: N-terminal kinase domain; PBD: polo-box domain; GlPLK1: *Giardia lamblia* PLK1; MT: microtubules; MTOC: microtubule-organizing center; GlCentrin: *Giardia lamblia* centrin; GlGAP1: *Giardia lamblia* glyceraldehyde 3-phosphate dehydrogenase; GlCENH3: *Giardia lamblia* centromeric histion H3

Declarations

Ethics approval and Consent to participate

Not applicable.

Consent for publication

Not applicable.

Availability of data and materials

Data supporting the conclusions of this article are included within the article and its additional files.

Competing interests

The authors declare that they have no competing interests.

Funding

This work was supported by National Research Foundation of Korea (NRF) grants funded by the Korea government (MSIT) (NRF-2020R1C1C1010581 to JK and NRF-2018R1D1A1A02085338 to SJP).

Authors' contributions

EAP, JK and SJP designed this study. EAP, JK and MYS performed the laboratory experiments. EAP, JK, and SJP analyzed and interpreted the data and wrote the manuscript. All authors read and approved the final manuscript.

Acknowledgements

We would like to thank Prof. Alexander R. Paredez (University of Washington), who provided the plasmid for transfection.

References

1. Elmendorf HG, Dawson SC, McCaffery JM. The cytoskeleton of *Giardia lamblia*. Int J Parasitol. 2003;33:3–28.
2. Markova K, Uzlikova M, Tumova P, Jirakova K, Hagen G, Kulda J, Nohynkova E. Absence of a conventional spindle mitotic checkpoint in the binucleated single-celled parasite *Giardia intestinalis*. Eur J Cell Biol. 2016;95:355–67.
3. Poxleitner MK, Dawson SC, Cande WZ. Cell cycle synchrony in *Giardia intestinalis* cultures achieved by using nocodazole and aphidicoliln. Eukayot Cell. 2008;7:569–74.
4. Reiner DS, Ankarklev J, Troell K, Palm D, Bernander R, Gillin FD, Andersson JO, Svärd SG. Synchronisation of *Giardia lamblia*: identification of cell cycle stage-specific genes and a differentiation restriction point. Int J Parasitol. 2008;38:935–44.
5. Horlock-Roberts K, Reaume C, Dayer G, Ouellet C, Cook N, Yee J. Drug-free approach to study the unusual cell cycle of *Giardia intestinalis*. mSphere. 2017;2:e00384-16.
6. Hardin WR, Li R, Xu J, Shelton AM, Alas GCM, Minin VN, Paredez AR. Myosin-independent cytokinesis in *Giardia* utilizes flagella to coordinate force generation and direct membrane trafficking. Proc Natl Acad Sci U S A. 2017;114:E5854–63.
7. Nigg EA, Stearns T. The centrosome cycle: Centriole biogenesis, duplication and inherent asymmetries. Nat Cell Biol. 2011;13:1154–60.
8. Thomas Y, Cirillo L, Panbianco C, Martino L, Tavernier N, Schwager F, Van Hove L, Joly N, Santamaria A, Pintard L, et al. Cdk1 phosphorylates SPAT-1/Bora to promote Plk1 activation in *C. elegans* and human cells. Cell Rep. 2016;15:510–8.
9. de Cárcer G, Manning G, Malumbres M. From Plk1 to Plk5: functional evolution of polo-like kinases. Cell Cycle. 2011;10:2255–62.
10. Sunkel CE, Glover DM. Polo, a mitotic mutant of *Drosophila* displaying abnormal spindle poles. J Cell Sci. 1988;89:25–38.
11. Fry AM, Bayliss R, Roig J. Mitotic regulation by NEK kinase networks. Front Cell Dev Biol. 2017;5:102.
12. Bruinsma W, Raaijmakers JA, Medema RH. Switching Polo-like kinase-1 on and off in time and space. Trends Biochem Sci. 2012;37:534–42.
13. Keister DB. Axenic culture of *Giardia lamblia* in TYI-S-33 medium supplemented with bile. Trans R Soc Trop Med Hyg. 1983;77:487–8.
14. Kim J, Shin MY, Park SJ. RNA-sequencing profiles of cell cycle-related genes upregulated during the G2-phase in *Giardia lamblia*. Korean J Parasitol. 2019;57:185–9.
15. Kim J, Nagami S, Lee KH, Park SJ. Characterization of microtubule-binding and dimerization activity of *Giardia lamblia* end-binding 1 protein. PLoS One. 2014;9:e97850.
16. Singer SM, Yee J, Nash TE. Episomal and integrated maintenance of foreign DNA in *Giardia lamblia*. Mol Biochem Parasitol. 1998;9:59–69.
17. Kim J, Park SJ. Roles of end-binding 1 protein and gamma-tubulin small complex in cytokinesis and flagella formation of *Giardia lamblia*. Microbiologyopen. 2019;8:e00748.
18. Carpenter ML, Cande WZ. Using morpholinos for gene knockdown in *Giardia intestinalis*. Eukaryot Cell. 2009;8:916–9.
19. Zhang J, Chengfu Y, Wu J, Elsayed Z, Fu Z. Polo-like Kinase 1-mediated phosphorylation of forkhead box protein M1b antagonizes its SUMOylation and facilitates its mitotic function. J Biol Chem. 2015;290(6):3708–19.

20. Gourguechon S, Cande WZ. Rapid tagging and integration of genes in *Giardia intestinalis*. Eukaryot Cell. 2011;10:142–5.
21. Kim J, Lee HY, Lee MA, Yong TS, Lee KH, Park SJ. Identification of α-11 giardin as a flagellar and surface component of *Giardia lamblia*. Exp Parasitol. 2013;135:227–33.
22. Colicino EG, Hehnly H. Regulating a key mitotic regulator, polo-like kinase 1 (PLK1). Cytoskeleton (Hoboken). 2018;75:481–494.
23. Lauwaet T, Smith AJ, Reiner DS, Romijn EP, Wong CC, Davids BJ, Shah SA, Yates JR 3rd, Gillin FD. Mining the *Giardia* genome and proteome for conserved and unique basal body proteins. Int J Parasitol. 2011;41:1079–92.
24. Golsteyn RM, Mundt KE, Fry AM, Nigg EA. (1995). Cell cycle regulation of the activity and subcellular localization of Plk1, a human protein kinase implicated in mitotic spindle function. J Cell Biol. 1995;129:1617–1628.
25. Wakida T, Ikura M, Kuriya K, Ito S, Shiroiwa Y, Habu T, Kawamoto T, Okumura K, Ikura T, Furuya K. The CDK-PLK1 axis targets the DNA damage checkpoint sensor protein RAD9 to promote cell proliferation and tolerance to genotoxic stress. Elife. 2017;6:e29953.
26. Pintard L, Archambault V. A unified view of spatio-temporal control of mitotic entry: Polo kinase as the key. Open Biol. 2018;8:180114.
27. Zitouni S, Nabais C, Jana SC, Guerrero A, Bettencourt-Dias M. Polo-like kinases: structural variations lead to multiple functions. Nat Rev Mol Cell Biol. 2014;15:433–52.
28. Bettencourt-Dias M, Rodrigues-Martins A, Carpenter L, Riparbelli M, Lehmann L, Gatt MK, Carmo N, Balloux F, Callaini G, Glover DM. SAK/PLK4 is required for centriole duplication and flagella development. Curr Biol. 2005;15:2199–207.
29. Bruinsma W, Aprelia M, Kool J, Macurek L, Lindqvist A, Medema RH. (2015). Spatial separation of Plk1 phosphorylation and activity. Front Oncol. 2015:5:132.
30. Kachaner D, Garrido D, Mehsen H, Normandin K, Lavoie H, Archambault V. Coupling of Polo kinase activation to nuclear localization by a bifunctional NLS is required during mitotic entry. Nat Commun. 2017;8:1701.
31. Wen D, Wu J, Wang L, Fu Z. SUMOylation promotes nuclear import and stabilization of Polo-like kinase 1 to support its mitotic function. Cell Rep. 2017;21:2147–59.
32. Li Z, Cui Q, Xu J, Cheng D, Wang X, Li B, Lee JM, Xia Q, Kusakabe T, Zhao P. SUMOylation regulates the localization and activity of Polo-like kinase 1 during cell cycle in the silkworm, *Bombyx mori*. Sci Rep. 2017;7:15536.
33. Gourguechon S, Holt LJ, Cande WZ. The *Giardia* cell cycle progresses independently of the anaphase-promoting complex. J Cell Sci. 2013;126:2246–55.
34. Kishi K, van Vugt MA, Okamoto K, Hayashi Y, Yaffe MB. Functional dynamics of Polo-like kinase 1 at the centrosome. Mol Cell Biol. 2009;29:3134–50.
35. Elia AE, Rellos P, Haire LF, Chao JW, Ivins FJ, Hoepker K, Mohammad D, Cantley LC, Smerdon SJ, Yaffe MB. The molecular basis for phosphodependent substrate targeting and regulation of Plks by the Polo-box domain. Cell. 2003;115:83–95.
36. Macurek L, Lindqvist A, Lim D, Lampson MA, Klompmaker R, Freire R, Clouin C, Taylor SS, Yaffe MB, Medema RH. Polo-like kinase-1 is activated by aurora A to promote checkpoint recovery. Nature. 2008;455:119–23.
37. Tavernier N, Panbianco C, Gotta M, Pintard L. Cdk1 plays matchmaker for the Polo-like kinase and its activator SPAT-1/Bora. Cell Cycle. 2015;14:2394–8.
38. Davids BJ, Williams S, Lauwaet T, Palanca T, Gillin FD. *Giardia lamblia* aurora kinase: a regulator of mitosis in a binucleate parasite. Int J Parasitol. 2008;38:353–69.
39. Kim J, Lee HY, Lee KH, Park SJ. Phosphorylation of Serine 148 in Giardia Lamblia End-binding 1 protein is important for cell division. J Eukaryot Microbiol. 2017;64(4):464–80.
40. Dawson SC, Sagolla MS, Mancuso JJ, Woessner DJ, House SA, Fritz-Laylin L, Cande WZ. Kinesin-13 regulates flagellar, interphase, and mitotic microtubule dynamics in *Giardia intestinalis*. Eukaryot Cell. 2007;6:2354–64.

Figures

Fig. 1

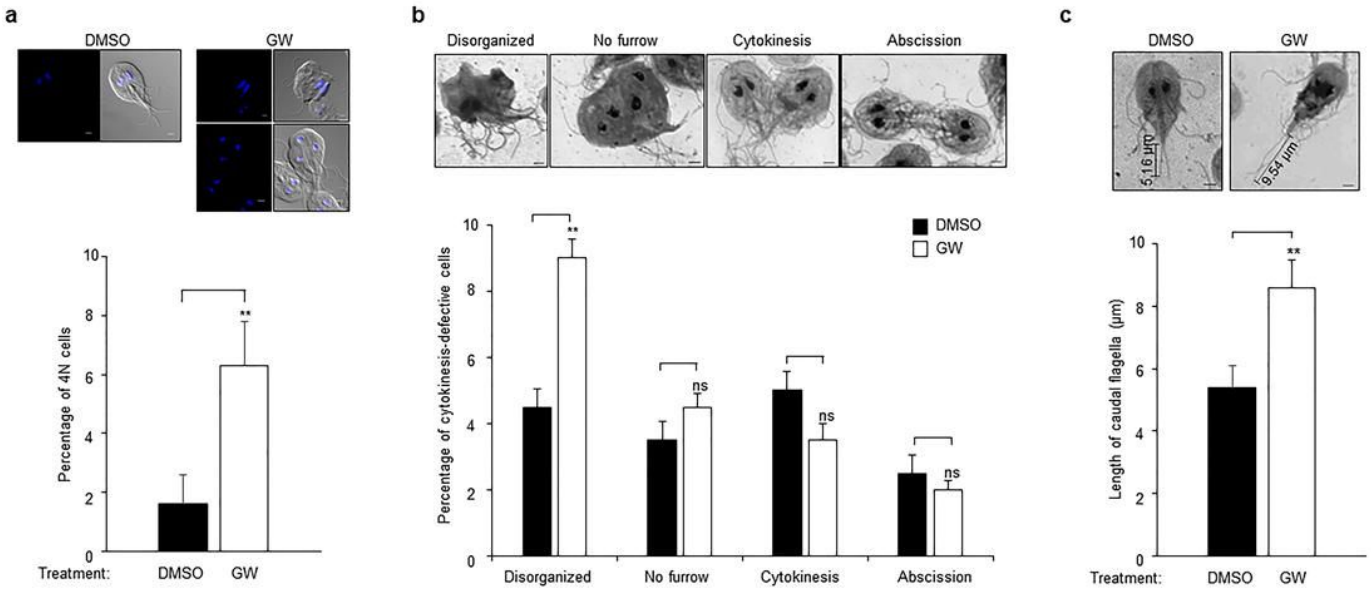

Figure 1

Effects of GW (5 μM), a PLK inhibitor on cytokinesis in G. lamblia. a Mitotic index. The cells were then mounted in VECTASHIELD Anti-fade Mounting Medium with DAPI. The numbers of cells with four or two nuclei were counted in 200 cells per condition. b Effects of GW on the numbers of Giardia cells at different stages of cell division. The cells were stained with 10% Giemsa solution, and observed with an Axiovert 200 microscope. c Effects of GW, a PLK inhibitor on flagella formation in G. lamblia. Giemsa staining was used to observe the effect of 5 μM GW on caudal flagella length using ZEN 2011. Caudal flagella length was measured in 200 cells per condition. The significance of differences among the conditions was evaluated using Student's t-tests. ** $P < 0.01$. Scale bars: 2 μm.

Fig. 2

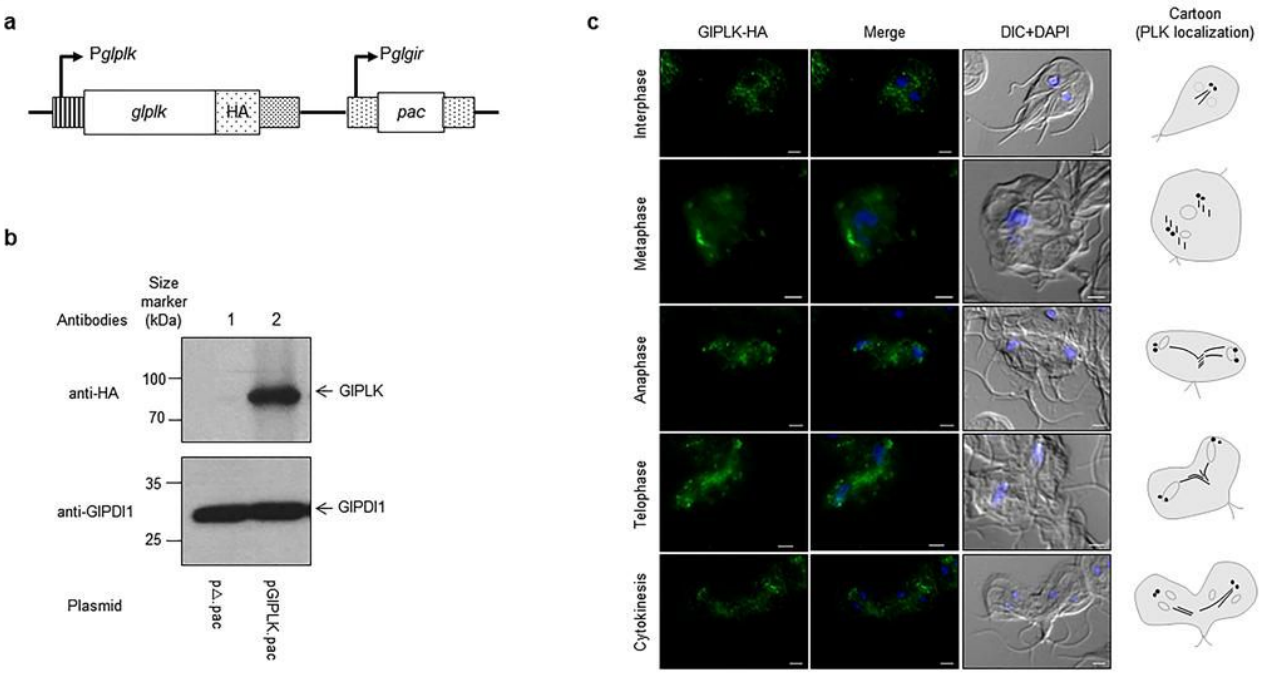

Figure 2

Expression and localization of GlPLK in G. lamblia-expressing HA-tagged GlPLK. a Schematic diagram of plasmid pGlPLK.pac. HA-tagged GlPLK was expressed from its own promoter, Pglplk. Transfected trophozoites were selected by puromycin resistance conferred by the pac gene expressed by the Pglgir promoter, a strong promoter of the 𝛫-giardin gene. As a control, Giardia trophozoites were also transfected with p𝛫.pac. b Western blotting to examine the expression of HA-tagged GlPLK. Extracts were prepared from G. lamblia containing p𝛫.pac (Lane 1) or pGlPLK.pac (Lane 2) and incubated with monoclonal mouse anti-HA antibodies. Membranes were incubated in stripping buffer, and then reacted with polyclonal rat antibodies specific to PDI1 of G. lamblia. c Localization of GlPLK. G. lamblia expressing HA-tagged GlPLK was probed with mouse anti-HA antibodies. The cells were then incubated with Alexa Fluor 488-conugated anti-mouse IgG. Slides were mounted with VECTASHIELD Anti-fade Mounting Medium with DAPI, and then observed with an Axiovert 200 fluorescent microscope. Scale bars: 2 μm.

Fig. 3

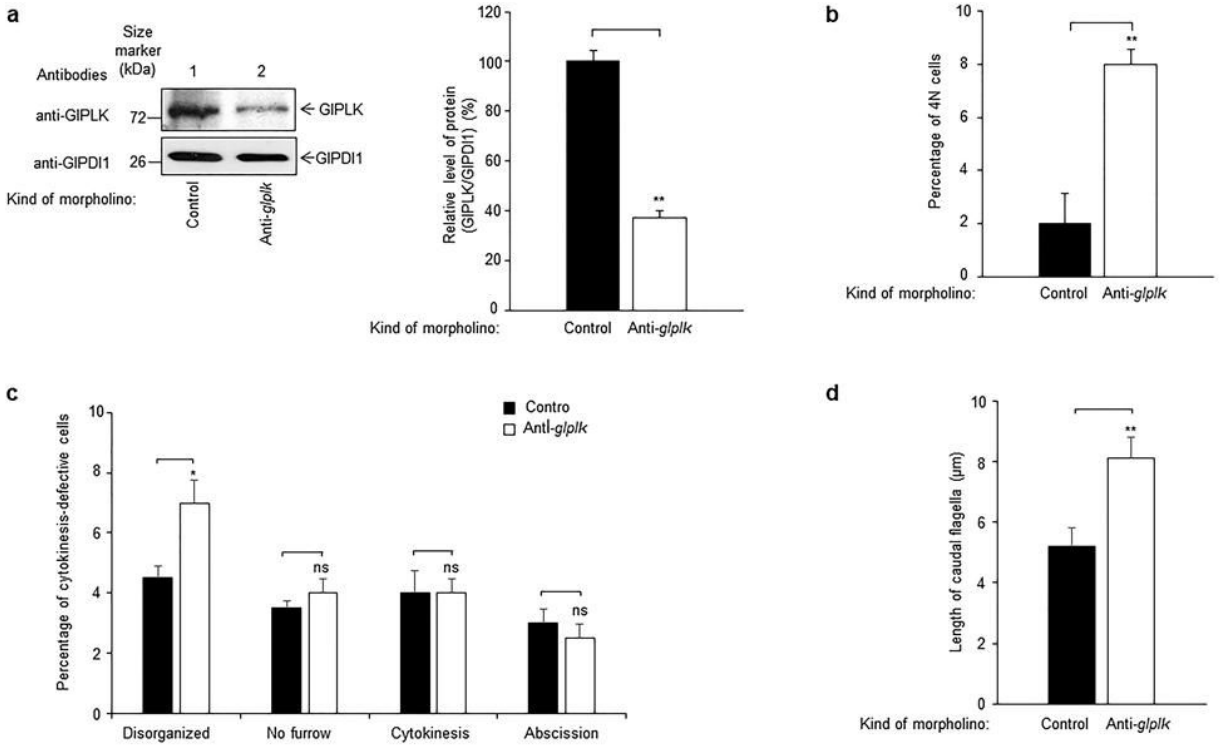

Figure 3

Morpholino-mediated knockdown of GlPLK expression in G. lamblia. Giardia trophozoites were collected at 24 h after electroporation with control or anti-glplk morpholino. a Cell extracts were analyzed by western blotting using anti-GlPLK or anti-GIPDI1 antibodies. The relative expression of GIPLK in cell extracts treated with anti-glplk morpholino compared to that of the control is presented as a bar graph. b Mitotic index of Giardia trophozoites transfected with control or anti-glplk morpholino. After Giemsa staining, cells with two or four nuclei were counted and then indicated in the graph as percentages. The percentage of the cell population was counted in 200 cells per condition and measured in triplicate for each sample. c The effect of GlPLK knockdown on cytokinesis was monitored by the following phenotypes: disorganized cytokinesis, defective furrow formation, defective cytokinesis, and failed abscission. d Effects of GlPLK knockdown on flagella formation in G. lamblia. The cells stained with Giemsa were used to measure caudal flagella length using ZEN 2011 (200 cells per condition). The significance of differences among the conditions was evaluated using Student's t-tests. *P < 0.05; **P < 0.01. Scale bars: 2 μm.

Fig. 4

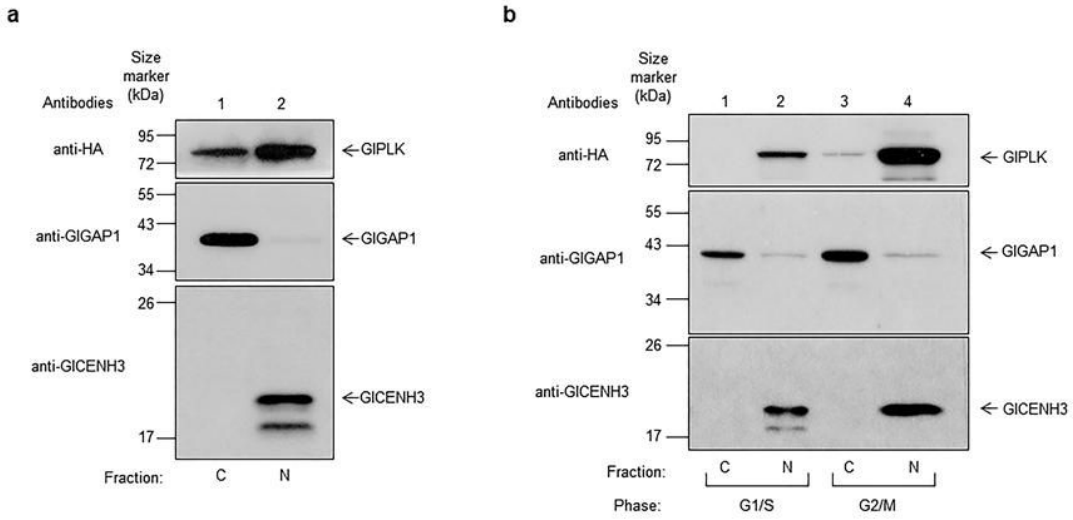

Figure 4

Nuclear localization of GlPLK in G. lamblia. Giardia carrying pGIPLK.pac was used to perform subcellular protein fractionation experiments. Both cytoplasmic and nuclear protein fractions were prepared from interphase, G1/S-phase, and G2/M-phase cells via sequential treatment with hypotonic and high-salt buffer. The amount of HA-tagged GlPLK in the extracts was monitored using anti-HA antibodies. The amount of GIGAP1, a cytoplasmic marker, was also detected using anti-GIGAP1 antibodies. As a marker for nuclear proteins, centromeric histone H3 was detected in theses extracts using anti-GICENH3 antibodies. a Western blotting of subcellular fractions derived from the interphase Giardia cells. Lane 1: cytoplasmic fraction (C); Lane 2: nuclear fraction (N). b Westrn blotting of subcellular fractions prepared from G1/S-phase and G2/M-phase cells. Lane 1, 3: cytoplasmic fraction (C); Lane 2, 4: nuclear fraction (N).

Fig. 5

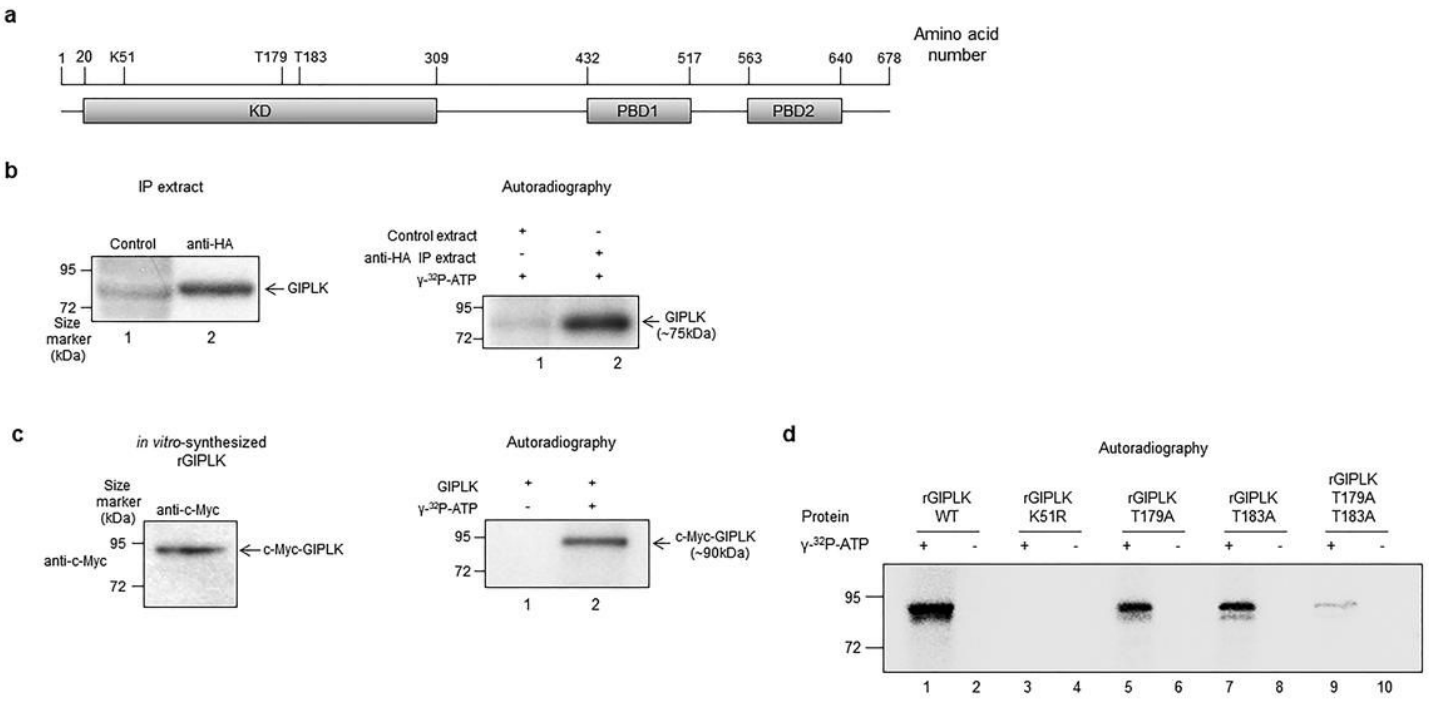

Figure 5

In vitro auto-phosphorylation of wild-type and mutant GIPLKs. a Schematic diagram of GIPLK. Serine/threonine kinase and two polo-box domains are indicated as boxes. Lys51 (K51) is suggested as a residue that initially receives phosphate from ATP, and two threonine residues (T179 and T183) are proposed as target sites of subsequent phosphorylation. b Phosphorylation of GIPLK in Giardia extracts IP with anti-HA antibodies. As a control, Giardia extracts were also precipitated with normal preimmune serum. For each kinase assay, IP extract was incubated with 2.5 μCi [-32P]ATP. c, d Phosphorylation of in vitro-synthesized GIPLKs. The c-Myc-tagged GIPLKs (wild type GIPLK, K51R mutant GIPLK and T179AT183A mutant GIPLK) were prepared in vitro and then used for kinase assays. GIPLK proteins were resuspended in 20 μL kinase buffer in the presence of 2.5 μCi [γ-32P]ATP. The kinase reactions were then subjected to 12% SDS-PAGE and visualized by autoradiography.

Fig. 6

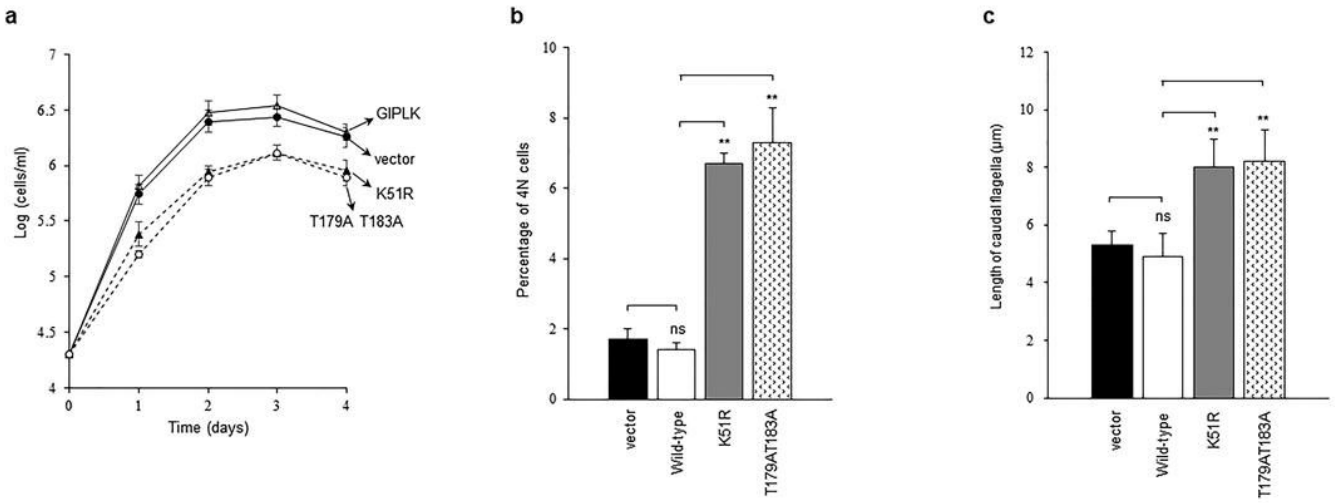

Figure 6

Functional defects caused by ectopic expression of mutant GlPLKs in Giardia. a Growth curves of Giardia carrying vector plasmid (closed circles) or expressing wild-type GlPLK (open triangles), K51R mutant GlPLK (closed triangles), or T178AT183A mutant GlPLK (open circles). The number of parasites per milliliter was determined using a hemocytometer. b Effects of mutant GlPLKs on cytokinesis in G. lamblia. Various Giardia cells (those carrying vector plasmid [closed bar], or expressing wild-type GlPLK [open bar], K51R mutant GlPLK [gray bar], or T178AT183A mutant GlPLK [dotted bar]) were stained with Giemsa in order to count the numbers of the cells with four nuclei. c Effects of mutant GlPLKs on flagella formation in G. lamblia. Giemsa staining was used to measure caudal flagella length using ZEN 2011 from 200 cells per condition. The significance of differences among conditions was evaluated using Student's t-tests. **P <0.01.

Supplementary Files

This is a list of supplementary files associated with this preprint. Click to download.

- supplement11.docx
- supplement12.tif
- supplement13.tif
- supplement14.tif
- supplement15.tif
- supplement16.tif
- supplement17.tif
- supplement18.tif
- supplement19.tif